CILAMCE 2017
Florianópolis - Santa Catarina - Brazil

EFFICIENCY OF BARS WITH FRACTAL POROSITIES SUBJECT TO MULTIPLE FUNCTIONS

Amanda Isabela de Campos

Marcelo Miranda Barros

amanda.campos@engenharia.ufjf.br

marcelo.barros@ufjf.edu.br

Structural Engineering Department, Federal University of Juiz de Fora, CEP 36036-330, Juiz de Fora, MG, Brazil

Abstract. *Natural systems have to deal with multiple functions, e.g. bones must withstand different loading conditions, absorb impact and exchange molecules such as blood cells. The geometry of bones presents a fractal character, that is self-similar porosity along scale. The high porosity renders light structures with high mechanical efficiency and internal surface area. A profound question is why nature develops fractal structures? In the present paper we compare geometric, structural and energetic properties of bars with different cross sections including simple hollow (unique hole), uniform porous (distributed holes with same size) and fractal porous (distributed holes with different sizes and quantities of each characteristic size) cross sections. The Sierpinski Carpet fractal pattern was used as reference geometry for the cross sections. The proposed beams are set to have the same material quantity. The properties investigated were: the internal surface area; stress and strain energy due to external pressure, bending and torsion within the linear elastic regime. Both analytical expressions and numerical simulations (FEM) were used to compare the proposed bars subject to each solicitation. The three proposed cross sections present high mechanical efficiency (stiffness/weight) in comparing with a filled bar. When subjected to pure bending or pure torsion the results show that the simple hollow beam is the best solution for minimizing stress, the worse for energy absorption and presents a very small relative surface area. Bars with uniform porosity are the best for energy absorption, possess high internal surface area but maximize stresses. Bars with fractal porosity present intermediate values for stress and energy absorption and possesses the highest internal surface area. However, under external pressure the simple hollow bar maximizes energy absorption, but also presents the highest concentration of stress. Once again the fractal section shows an intermediate behavior between the simple hollow beam and the one with uniform porosity. Then we concluded that fractal porosity is a good solution for structures subject to multiple functions, including different solicitations and exchanging of energy (impact and heat for example).*

Keywords: *multi-scale porosity, mechanical efficiency, multiobjective optimization*

INTRODUCTION

Nature builds efficient and multifunctional structures in both plants and animals (Liu and Jiang, 2011). Porous structures are lightweight multifunctional structures with high internal surface areas in order to exchange entities as occurs in trees and bones (Ashby, 1983; Malshe et al., 2013). Besides dealing with support, natural biological structures have to deal with transport of water, nutrients, residues etc. The underlying geometries of such structures are complex and oftentimes present self-similar patterns (Song et al., 2005). Natural optimization results from changing and adaptation along many thousands of years, where structures are subject to many situations and must attend many functions (Thompson, 1961).

Mechanical efficiency may be defined as a measure of how an object is able to support external forces without collapsing and at the same time presenting low weight. Disregarding the material properties and focusing on the form, low weight means spending less material in constructing and less energy in moving the structure. Examples of mechanically efficient natural objects are timber and bones. Metal foams are man-made efficient structures with the following characteristics: high impact absorption, sound absorption, electromagnetic shielding and vibration damping (Ashby et al., 2000).

The concept of stiffness is related to how much a structure resists deformations when subjected to forces, which is the inverse of flexibility. In several situations it is interesting that a bar has high stiffness. Stiffnesses are measures of how good a structure is to transport forces or moments. In terms of cross section geometries the flexural stiffness is given by the second order moment with relation to the bending axis. Then, in order to increase the flexural stiffness it is necessary to increase the distance of the area to the bending axis. The "I" sections, for example, are widely used because they have a high flexural stiffness with relation to the horizontal axis, thus, minimizing the values of the normal strains and stresses due to bending moment. On the other hand the “I” sections are not adequate to resist torsion since the second order moment with relation to the bar axis is relatively small. That is the “I” section is largely used to resist bending in one direction and the related undesired phenomena due to second order effects must be considered.

Fractal geometry consists in a mathematical description of complex geometries, commonly self-similar ones. Mandelbrot (1982) proposed that umpteen natural forms may adequately be modelled by fractal geometry. A vast range of fractal geometries may be generated by simple rules and recursiveness. In general the patterns in fractal geometries resemble geometries of natural objects and the fractal dimension has been largely used as a measure for patterns observed in diverse phenomena (Feder, 1988). The computers as well as the 3D printing technologies permit us to model, simulate, generate and experiment the behavior of structures with complex forms (Obaldia et al., 2015).

Bar structures may be subject to multiple solicitations (Anwar, 2017) as compression, traction, bending, twisting and impact, e.g. in trees and long bones. In the present paper we compared geometric as well as mechanical properties of straight prismatic porous bars with same volume but different forms. Three classes of geometries for the cross sections which provide efficient structures were compared, namely fractal porosity, homogeneous porosity and single hollow. The bars were subjected to bending, torsion and external pressure.

Kirkhope et al. (2012) have shown that the weight of space frames can be reduced if they are designed using a hierarchical pattern. The researchers have worked out a way to calculate an optimal “hierarchical structure” built from a certain material so that it can withstand a given load. They claim that using such techniques could help in building highly efficient load-bearing structures that could be used in solar sails, cranes or other lightweight-yet-strong constructs.

Recent works have shown that through the use of porous design, high mechanical efficiency can be obtained for structures (Kirkhope et al., 2011; Farr and Mao, 2008; Farr, 2007; Murphey and Hinkle, 2003). Experimentals work on hierarchical sandwich panels has confirmed theoretical predictions that second order panels exhibit strength ten times greater than their first order counterparts of the same relative density (Kooistra et al., 2007).

By combining 3D printing technique, numerical analysis, and experiments to design a new class of sandwich composites Li and Wang (2017); Li and Lu (2015) three-point bending tests are performed to investigate the bending behavior of these composites. Under bending deformation, sandwich composites provide higher flexural stiffness and strength that are desirable in several structures. The experimental and numerical results indicate that architected core structures can be utilized to tailor the bending properties as well as failure mechanisms and one significantly enhances in the energy absorption abilities. Webman (1986) affirms in his study that fractal objects are good for resisting external pressure.

1 Porous bars subject to multiple functions

Bars are long elements with relatively small cross section size. Consider bars with same length *L* following three different patterns for their cross sections which evolve iteratively. The three classes of proposed geometries are the following: fractal porosity (based on the Sierpinski carpet), uniform porosity and single hollow. Each class of geometries evolves with parameter *k*. In fact, for each evolution step in the Sierpinski class is associated a homogeneous porous beam and a single hollow beam with same volume. Thus, for each iterative step the three different beams present the same volume and weight. Figure 1 shows the cross sections for the three patterns (columns) and the corresponding iterations k (rows) until order three. The three families of cross sections become very efficient while evolving and to the best of our knowledge the proposed approach have not been presented yet.

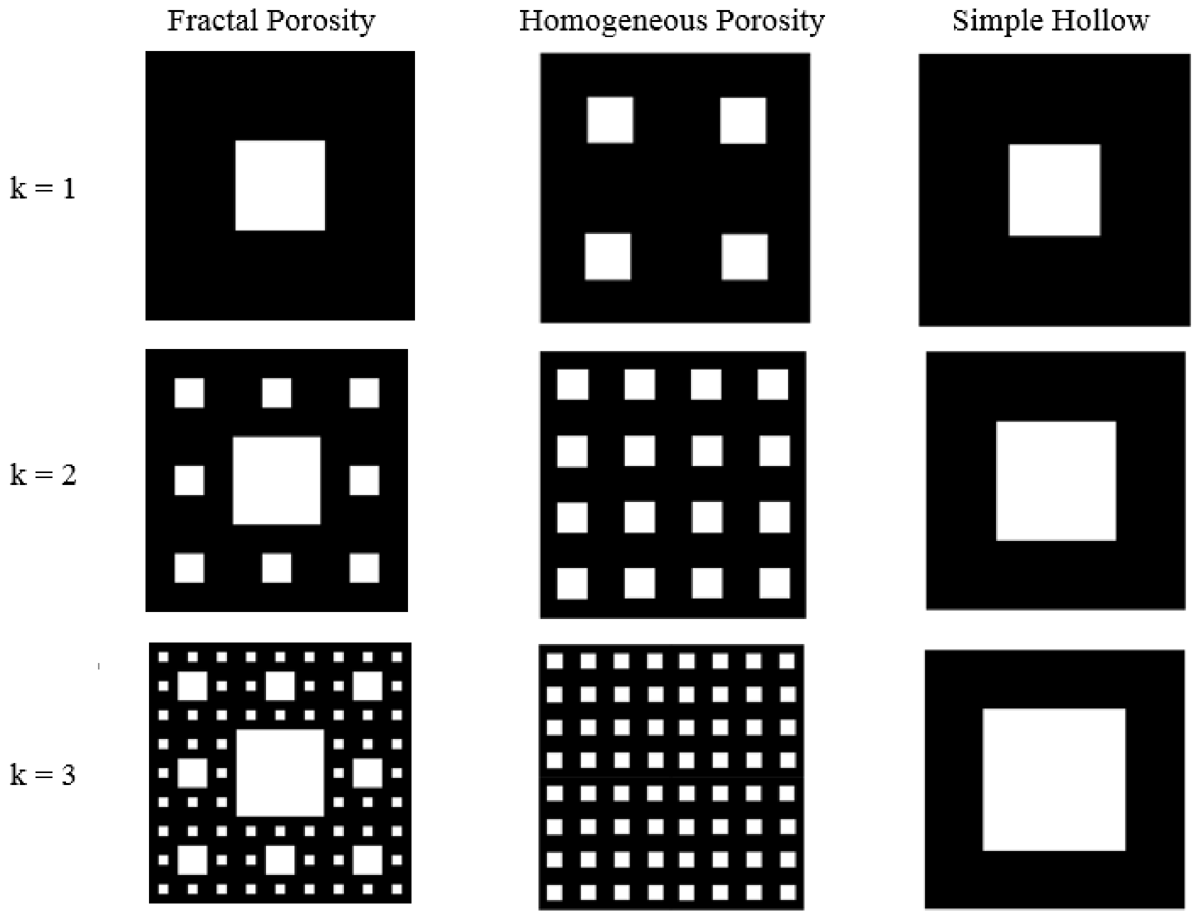

Figure 1. Sequences of cross sections for the three classes of geometries, namely fractal porosity, homogeneous porosity and single hollow

We investigate the total internal surface area, mechanical efficiency in bending, stresses and elastic energy within bars when subject to external pressure, bending and torsion considering the linearly-elastic regime.

1.1 Geometric properties: cross section area, cross section moment of inertia and internal surface area

The geometrical properties of the cross sections, for each class, are determined as functions of a characteristic length λ_k as illustrates Figure 2.

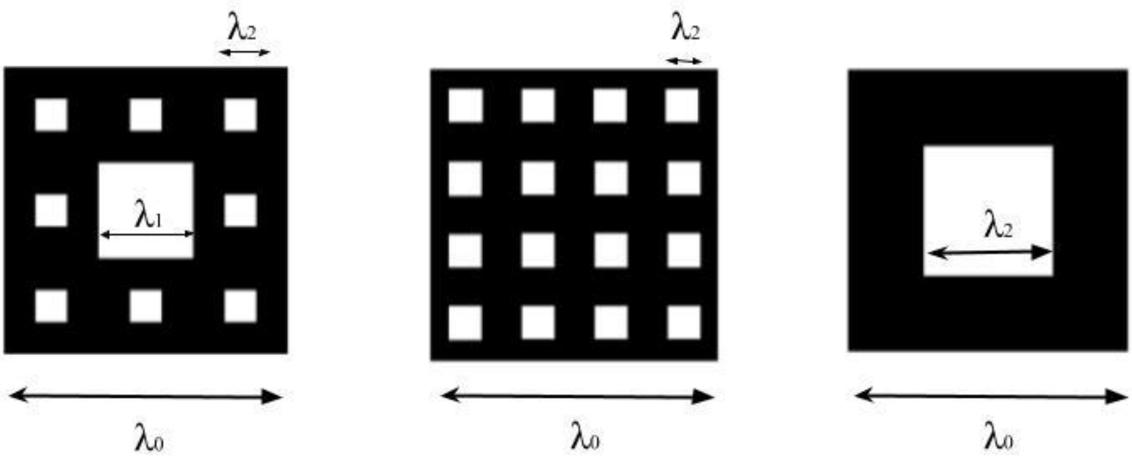

Figure 2. Characteristic measures for the cross sections at 2nd order

1.1.1 Sierpinski Carpet (fractal) sequence

As benchmark for the fractal cross section we used the Sierpinski carpet pattern. The Sierpinski carpet is build up through an iterative process by dividing a square into nine other similar squares, removing the central square and retaining the other eight ones. The procedure is repeated indefinitely and as limit a fractal geometry is obtained (Feder, 1988). Thus each square at order k gives rise to eight squares reduced by factor three.

The kth order term in the Sierpinski Carpet is composed of $N_k = 8^k$ squares of side $\lambda_k = \lambda_0 3^{-k}$ where λ_0 is the length of the outer side of the square. Then, the relative cross section area of a Sierpinski carpet of term k is:

$$\frac{A_k}{A_o} = N_k \left(\frac{\lambda_k}{\lambda_0}\right)^2 = \left(\frac{8}{9}\right)^k, \tag{1}$$

where A_0 is the cross section area of the filled square. Note that the total cross section area as well as the volume tend to zero with evolution, i.e. increasing k.

On the other hand, as the number of holes increases the internal surface area also increases with evolution. The internal surface area can be determined by the perimeter of the holes times the length of the bar. The total surface area of a bar with a Sierpinski carpet pattern for the cross section is given by:

$$S_k = \frac{4}{3}\sum_{n=0}^{k-1}\left(\frac{8}{3}\right)^n L\lambda_0 \tag{2}$$

which tends to infinity with evolution.

For the calculation of the second order moment (usually called moment of inertia) in a kth order term, with respect to the horizontal axis passing through its centroid, it is necessary to use the parallel-axis theorem (Steiner's theorem). Then the cross section moment of inertia of order k is obtained as:

Proceedings of the XXXVIII Iberian Latin-American Congress on Computational Methods in Engineering
P.O. Faria, R.H. Lopez, L.F.F. Miguel, W.J.S. Gomes, M. Noronha (Editores), ABMEC, Florianópolis, SC, Brazil, November 5-8, 2017.

$$I_k = \int_A y^2 dA = \sum_{i=1}^{N_k} \left(\bar{I}_k + \bar{A}_k \, y_{i,k}^2 \right) = N_k \frac{\lambda_k^4}{12} + \lambda_k^2 \sum_{i=1}^{N_k} y_{i,k}^2 \,, \tag{3}$$

where $\bar{I}_k$ is the moment of inertia of each square with relation to their own centroid, $\bar{A}_k$ is the area of the corresponding squares and $y_{i,k}$ are the distances between the global centroid and the axis passing through the centroid of each square *i* at order *k*. The relative moment of inertia is then:

$$\frac{I_k}{I_0} = N_k \left(\frac{\lambda_k}{\lambda_0} \right)^2 \left[\left(\frac{\lambda_k}{\lambda_0} \right)^2 + \Omega_k \right] = \left(\frac{8}{9} \right)^k \left[\left(\frac{1}{9} \right)^k + \Omega_k \right], \tag{4}$$

where $\Omega_k = 12 \left[\sum_{i=1}^{N_k} \left(\frac{y_{i,k}}{\lambda_0} \right)^2 \right] / N_k$ takes into account the spatial distribution of the squares in vertical direction. It is clear that the moment of inertia tends to zero with evolution, since the cross section area tends to zero also. As $\Omega_k \to C$ (constant), $I_k / I_{k-1} \to 8/9$ as $k \to \infty$, i.e. the ratio of consecutives moments of inertia tends asymptotically to 8/9. Note that the relative cross section areas follow the same ratio $A_k / A_{k-1} \to 8/9$ for all *k*.

1.1.2 Homogeneous porosity sequence

The construction of the sections called homogeneous porosities follows the pattern that each hole gives rise to another four in the next order. Thus the number of holes in each order is $N_k = 4^k$. The size of the holes are determined in such a way that the total cross section area coincides with the corresponding order of the Sierpinski bar. Thus,

$$A_k = \left(\frac{8}{9} \right)^k A_0 = A_0 - 4^k \lambda_k^2 \Rightarrow \lambda_k = \sqrt{\frac{A_0}{4^k} \left(1 - \left(\frac{8}{9} \right)^k \right)}, \tag{5}$$

The internal surface area is obtained as the perimeter of all holes times the length of the beam obtained simply as:

$$S_k = 4^{k+1} \lambda_k L \,. \tag{6}$$

The moment of inertia of the section with equal holes may be obtained by subtracting the moment of inertia of the small squares with relation to the filled section (the moment of inertia of each hole is obtained with equation (3)). For the *k*th order term the moment of inertia is given by:

Proceedings of the XXXVIII Iberian Latin-American Congress on Computational Methods in Engineering
P.O. Faria, R.H. Lopez, L.F.F. Miguel, W.J.S. Gomes, M. Noronha (Editores), ABMEC, Florianópolis, SC, Brazil, November 5-8, 2017.

$$I_k = \frac{\lambda_0^4}{12} - 4^k \left(\frac{\lambda_k^4}{12} \right) - \sum_{n=1}^{2^{(k-1)}} \left(2^{(k+1)} \left[\lambda_k (2n-1) \left(\lambda_k^{'} + \frac{\lambda_k}{2} \right) \right]^2 \right), \tag{7}$$

where $\lambda_k^{'} = (\lambda_0 - 2^k \lambda_k) / 2^{k+1}$ is the side of the squares not removed.

1.1.3 Single hollow sequence

The hole size of the single hollow section is determined in such a way that the cross section area is equal to the corresponding *k*th order term of the Sierpinski sequence.

$$A_k = \left(\frac{8}{9} \right)^k A_0 = A_0 - \lambda_k^2 \Rightarrow \lambda_k = \sqrt{A_0 \left(1 - \left(\frac{8}{9} \right)^k \right)} . \tag{8}$$

The internal surface area can be calculated as the perimeter of the hole times the length of the beam, expressed as:

$$S_k = 4 \lambda_k L . \tag{9}$$

The moment of inertia of a single hollow section is easily obtained as the moment of inertia of the filled section minus the moment of inertia of the hole, i.e.:

$$I_k = \frac{\lambda_0{}^4}{12} - \frac{\lambda_k{}^4}{12} = \frac{\lambda_0{}^4}{12} - \frac{\sqrt{\lambda_0{}^2 \left(1 - \left(\frac{8}{9} \right)^k \right)}}{12} . \tag{10}$$

The internal surface area of the simple hole section is given by $S_k = 4 \lambda_k L$ which tends to the limit value of $S_k = 4 \lambda_0 L$.

Figure 3 shows the internal surface areas (a) and moments of inertia (b) for the three classes of geometries along iterations until the 10th order terms. Note that the fractal Sierpinski sequence presents the highest internal surface area, followed by the homogeneous porosity, both increasing exponentially, whereas the single hollow sections presents a very limited internal surface area given by $4 \lambda_0 L$. Note that the single hollow section presents the highest cross section moment of inertia, followed by the fractal porosity and then the homogeneous porosity.

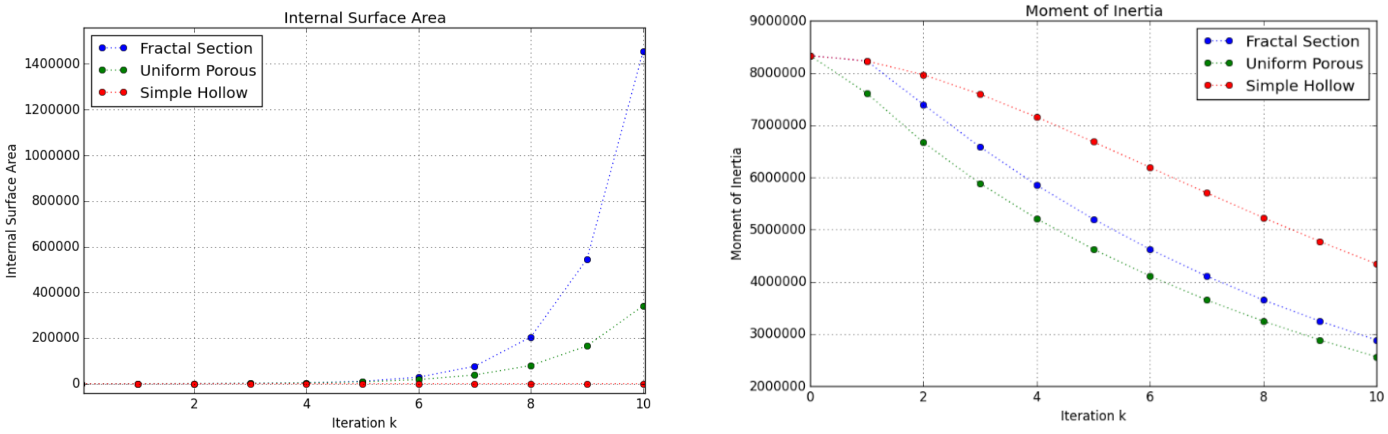

(a) (b)

Figure 3: Internal surface area (a) and moments of inertia (b) for the three classes of geometries varying with evolution until the 10th order term. ($\lambda_0 = 100$, L=1)

It can be observed that the section of Sierpinski up to the third order loses in internal surface area for the section of uniform porous, however the Sierpinski beam has a tendency of superior growth and from the fourth order on it surpasses the sections of equal holes and coffin with relation to this property.

1.2 Cross section efficiency in bending due to geometry

We define the cross section bending efficiency due to geometry for an order k is defined as:

$$e_k = C \frac{I_k}{A_k{}^2}, \; k=0,1,... \tag{11}$$

Then the efficiency is defined as the ratio between the cross section moment of inertia and the corresponding cross section area squared. Thus the efficiency is a dimensionless quantity and C = 12 so as the efficiency of the filled section equals unity. Figure 8 shows the flexural efficiencies for the three classes of geometries along evolution.

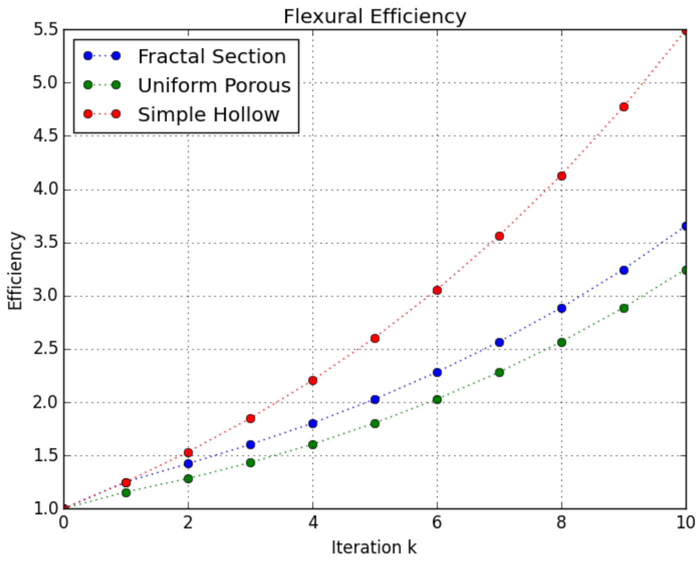

Figure 4: Flexural efficiencies with evolution.

It is clear that the simple hollow class presents the highest efficiencies while not considering the effects of second order as local buckling. The fractal sections present higher efficiencies than those of the homogeneous porosities.

1.3 Porous bars subject to bending, torsion and external pressure

The three classes of bars are now tested through numerical simulations subject to bending moment, torsion moment and external pressure, considering the component material as isotropic within the linearly elastic regime. The presented mechanical properties are the maximum stress and the strain energy. The maximum stress is a local property whereas the elastic energy depends on the intensity of the stresses and is a global property. On one hand the maximum normal stress due to a bending moment M is given by $\sigma_{\max} = 6M\lambda_0^{-3}$ and the maximum shear stress due to a torsion moment T is approximately given by $\tau_{\max} = 7.11T\lambda_0^{-3}$ for a filled squared section. The strain energies U due to pure bending and pure torsion are easily obtained, given respectively by $U_{bending} = M^2L/(2EI)$ *and* $U_{torsion} = T^2L/(2GJ)$ where E and G are the longitudinal and the transversal elastic moduli; I and J are the moment of inertia with relation the horizontal axis passing through the centroid and the torsional constant; M and T are the bending and torsion moments.

In order to validate the numerical results we compared analytical and numerical results for the maximum stresses as well as the strain energies due to bending and torsion for a squared filled section. The results are shown in table 1.

Table 1: Comparison between analytical and numerical results for maximum stress and strain energy of a filled square section bar subject to pure bending or pure torsion. Parameters: E=210GPa, ν = 0.3, λ_0 = 10cm, L=50cm. M and T are set to provide the same maximum stress.

	Bending		Torsion	
Filled square section	Strain energy	Maximum stress	Strain energy	Maximum stress
Analytical	0.00474	1.093	0.005199	1.093
Numerical	0.00471	1.152	0.005176	1.171
Relative Difference	0.56%	5.40%	0.43%	7.14%

2 Numerical results

The three classes of geometries shown in Figure 1 until the third order term are considered as cross sections for bars with same length and solicited by pure bending, torsion or external pressure. The considered values for properties are: E=210GPa, ν = 0.3, λ_0=10cm, L=50cm. The boundary conditions and the corresponding results of stresses (von Mises) for the third order term in each class are shown in Figures 5 (bending), 6 (torsion) and 7 (external pressure).

The numerical results were obtained using the software Abaqus/CAE and the finite element type used for the bars were three-dimensional hexahedral element, called C3D8R which means Continuum, 3-D, 8-node and reduced integration. For the plane state two-dimensional quadrilateral elements were S4R: Shell, 4-node and reduced integration.

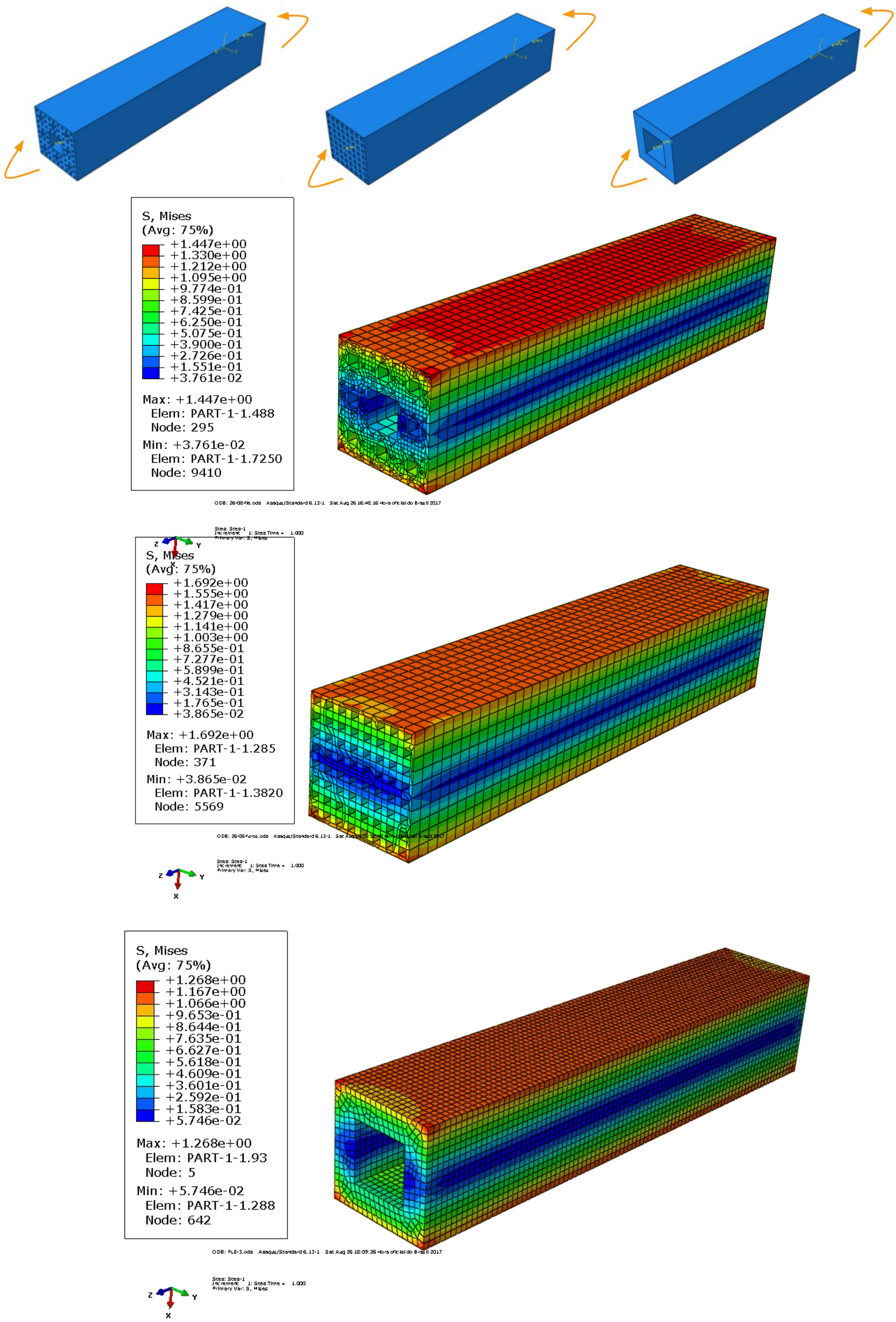

Figure 5. Boundary conditions and stress distributions (von Mises) considering the bending solicitation for the three geometries at *k*=3

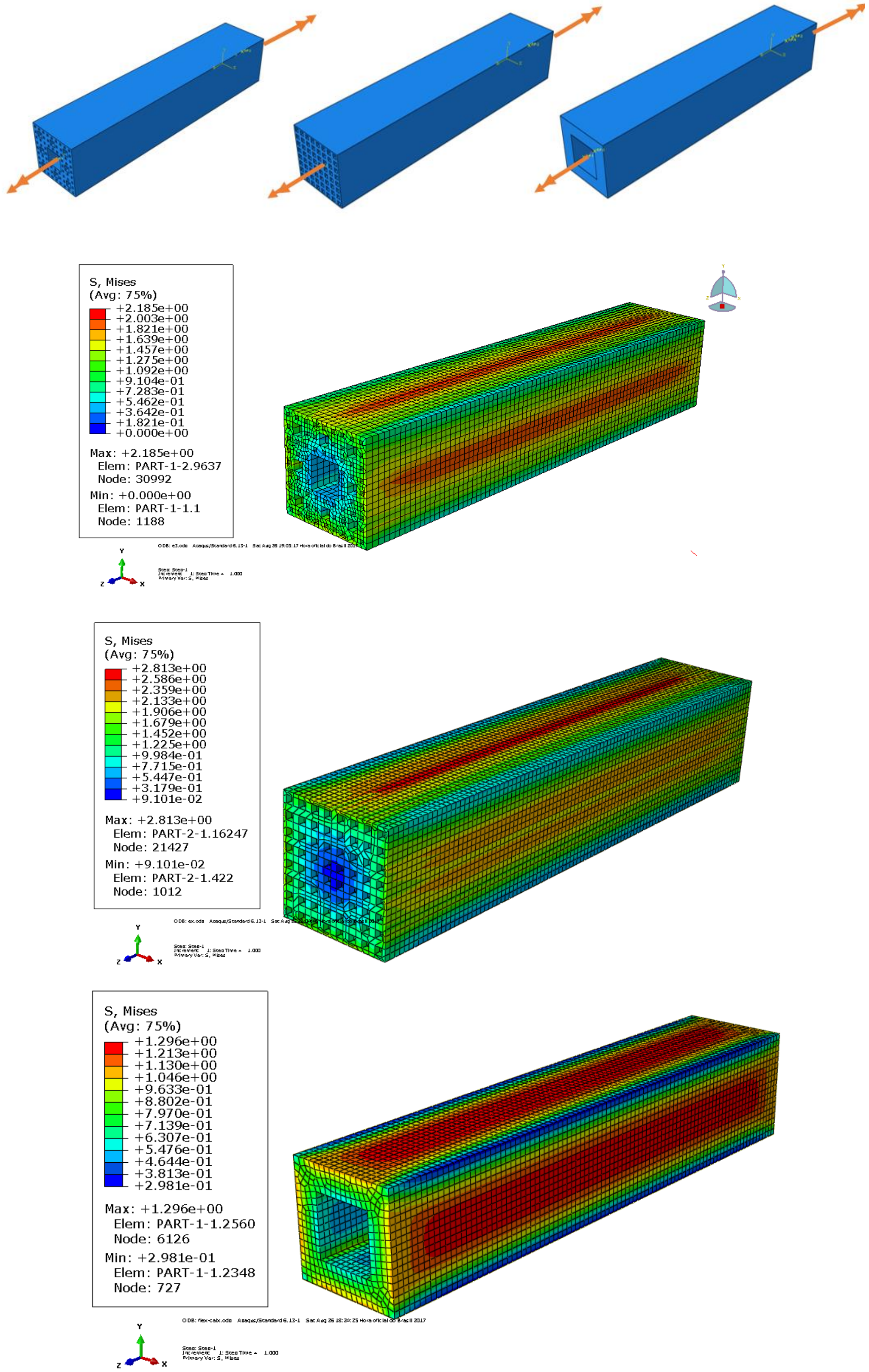

Figure 6. Boundary conditions and stress distributions (von Mises) considering the torsion solicitation for the three geometries at *k*=3

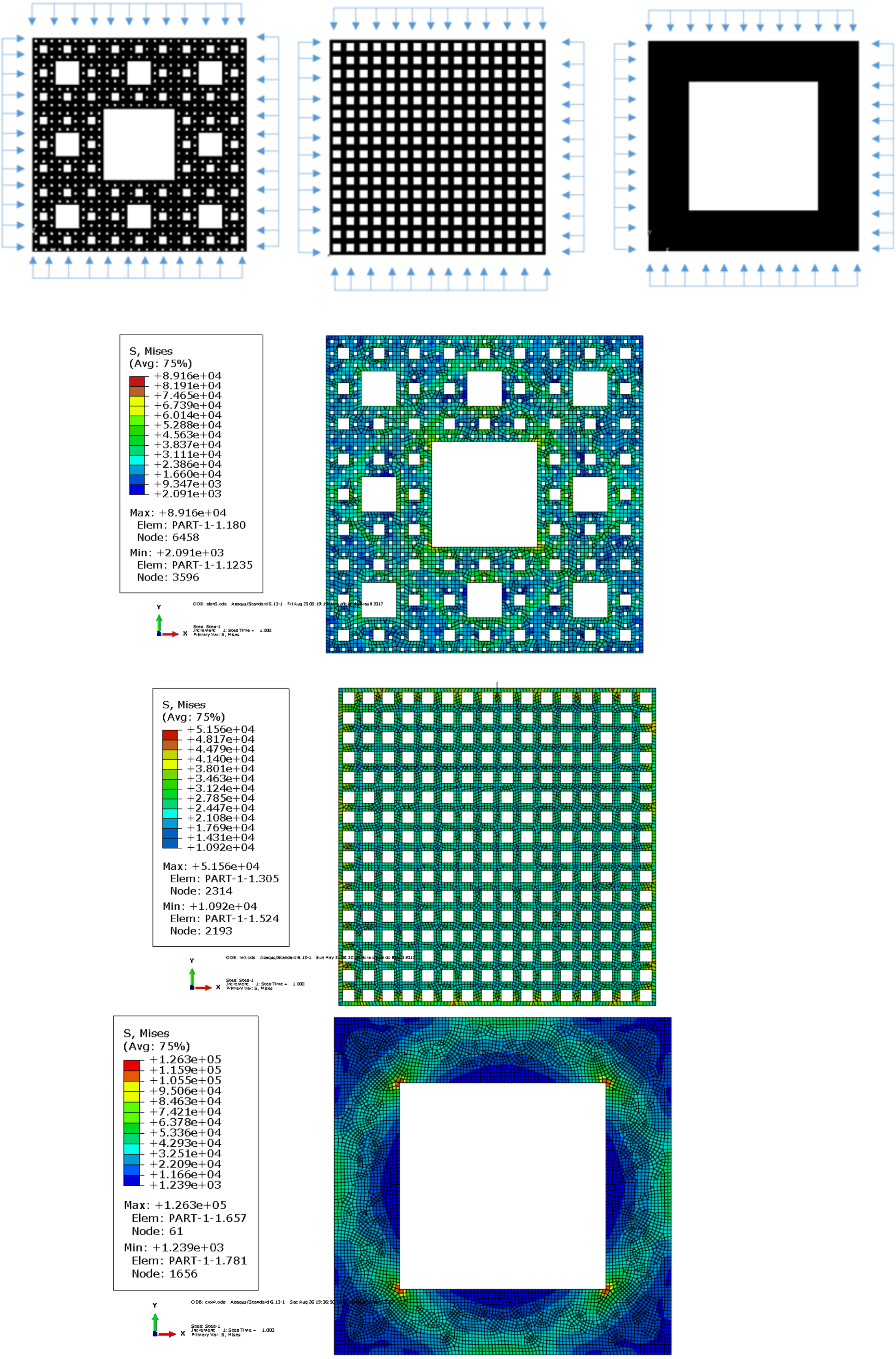

Figure 7. Boundary conditions and stress distribution (von Mises) considering the external pressure solicitation for the three geometries at *k*=3

Figure 8 shows the values of maximum stresses as well as strain energies as functions of evolution k for the three solicitations. Each graph shows the mechanical results for the bars with cross section geometries given by the three classes of geometries, namely fractal porous, uniform porous and simple hollow.

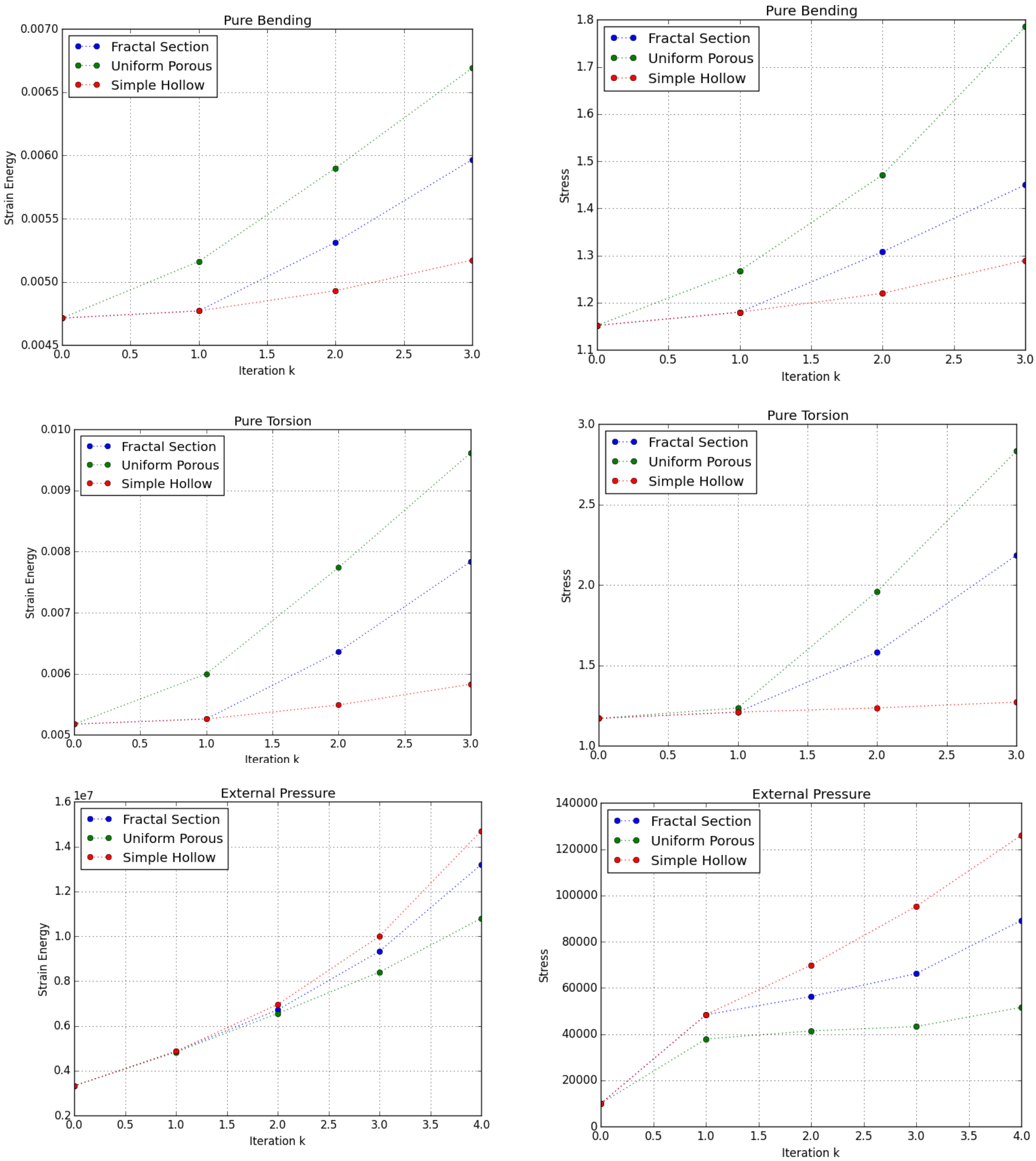

Figure 8. Stresses and strain energies considering the three solicitations over the three first order terms of the three classes of geometries

3 Conclusions

The proposed analysis consisted in comparing geometrical and mechanical properties for the three proposed classes of cross section geometries for bars. Corresponding bars at the same evolution k have the same cross section area, volume and weight. The cross section areas tend to zero with evolution, according to expression (1). The cross section moments of inertia also tend to zero and are illustrated in Figure 3(b) where the simple hollow class presents higher moments of inertia followed by the fractal and then followed by the homogeneous porosities classes.

The internal surface areas increase with evolution for the three classes, as Figure 3(a), but while for the simple hollow class it tends to a small limited value, for uniform and fractal porosities the internal surface areas increase without bound exponentially. Further, the fractal porosity class presents a higher growth rate than the uniform porosity for the internal surface area yielding a much higher internal surface area for advanced evolution.

It is defined the flexural efficiency due to geometry of a cross section as the ratio between its moment of inertia and its area squared, by expression (2). Higher efficiencies means higher relation stiffness/weight. The single hollow class presents the higher flexural efficiency, followed by the fractal and then the homogeneous porosities. Note that fractal and homogeneous porosities are multicelled and then the consideration of the second order effects may lead them to be better than the thin simple walled section obtained by the single hollow class.

It was found that from a mechanical point of view all proposed classes are very efficient solutions. Simple hollow class is the best, among the three, for resisting bending and torsion but the worst for resist external pressure. Homogeneous porosity class is the best for resisting external pressure and the worst in bending and torsion. Fractal porosity class is the intermediate solution for the three proposed mechanical functions. That is for bars subject to those multiple functions the fractal porosity is the most balanced solution.

A larger internal surface area may be associated with some phenomena of transport through surface as exchange of heat or substances. Nature abounds with porous structures with very high internal surface areas. Tissues are composed of a countless quantity of cells, each of which needs to be fed and deliver their residues. Thus the problem of transport through surface is of great importance in living things in order to sustain each cell and then the whole organism.

An advantage of bars with longitudinal porosity is for using them to transport fluids, by using circular porous. For fluid transport the simple hollow beam with circular cross section presents the best solution for one fluid flow in terms of velocities since it presents the highest relative tube diameter. The homogeneous and fractal porosities present a quantity of ducts that may be used to transport more than one fluid in both directions, with lower velocities according to the sizes of the holes. The fractal porosity presents a range of sizes for the tubes which may be used for more diverse situations. The present paper proposes and analyzes straight unidimensionaly porous bars in a way we have not seen before. The results indicate that fractal porosity, largely found in nature, may be optimum in dealing with multiple functions, where we considered only some possible ones.

Possible applications for the proposed geometries are in members of buildings, robots, aircrafts and spacecrafts, providing light efficient structures with internal transport of charges and fluids.

ACKNOWLEDGEMENTS

We thank FAPEMIG (Foundation for Research Support of the State of Minas Gerais) for giving us the support to attend the conference.

REFERENCES

Anwar, N., Najam, F. A., "*Structural Cross-Sections: Analysis and Design*", BH Elsevier, 2017.

Ashby, M.F., "*The Mechanical Properties of Cellular Solids*", Metallurgical Transactions A, 14A, 1755-1769, 1983.

Ashby, M.F., Evans, A., Fleck, N.A., Gibson, L.J., Hutchinson, J.W., Wadley, H.N.G., "*Metal foams: A Design Guide*", BH Elsevier, 2000.

Farr, R.S., Mao, Y., *"Fractal space frames and metamaterials for high mechanical efficiency",* EPL (Europhysics Letters), 2008.

Feder, J., "*Fractals*", Springer, 1988.

Kirkhope, D. R., et al., *"Hierarchical Space Frames for High Mechanical Efficiency: Fabrication and Mechanical Testing,"* Mech. Res. Commun. 46, 41, 2012.

Kooistra, G.W., Deshpande, V., Wadley, H.N.G., "*Hierarchical Corrugated Core Sandwich Panel Concepts"*. J. Appl. Mech. 74, 259–268., 2007.

Li, T., Wang, L., "*Bending behavior of sandwich composite structures with tunable 3D-printed core materials",* Composite Structures, Volume 175, 1 September, Pages 46-57, 2017.

Li, Z., Lu, F., *"Bending resistance and energy-absorbing effectiveness of empty and foam-filled thin-walled tubes",* Journal of Reinforced Plastics and Composites, 2015.

Liu, K., Jiang, L., "*Bio-inspired design of multiscale structures for function integration*", Nano Today, 6, 155-175, 2011.

Malshe, A., Rajurkar, K., Samant, A., Hansen, H.N., Bapat, S., Jiang, W., "*Bio-inspired functional surfaces for advanced applications*", CIRP Annals - Manufacturing Technology, 62:2, 607-628, 2013.

Mandelbrot, B.B., "*The Fractal Geometry of Nature*", W. H. Freeman and Co., New York, 1982.

Murphey, T.W., Hinkle, J.D., "*Some performance trends in hierarchical truss structures"*. In: Proc. 44th Structures, Structural Dynamics and Materials Conf. p.2003-1903, 2003.

Obaldia, E.E., Jeong, C., Grunenfelder, L.K., Kisailus, D., Zavattieri, P., "*Analysis of the mechanical response of biomimetic materials with highly oriented microstructures through 3D printing, mechanical testing and modeling*", J. of the Mech. Beh. of Biomed. Mat., 48, 70-85, 2015.

Song, C., Havlin, S., Makse, "*Self-similarity of complex networks*", Letters to Nature, 433, 392-395, 2005.

Thompson, D.W., "*On Growth and Form*", Cambridge University Press, 1961.

Webman, I., "*The Elastic Behavior Of Fractal Structures",* In Fractals in Physics, Elsevier, Amsterdam, Pages 343-349, 1986.